

Structure of Zinc Phosphate Glasses of 75 and 80 mole% ZnO Content Studied by X-Ray Diffraction and Reverse Monte Carlo Simulations

Uwe Hoppe^a, Yanko Dimitriev^b, and Pal Jóvári^{c,d}

^a Universität Rostock, Institut für Physik, Universitätsplatz 3, D-18051 Rostock, Germany

^b University of Chemical Technology and Metallurgy, Department of Silicate Technology, 8 Kl. Ohridski Blvd., 1756 Sofia, Bulgaria

^c Hamburger Synchrotronstrahlungslabor HASYLAB am Deutschen Elektronen-Synchrotron DESY, Notkestr. 85, D-22607 Hamburg, Germany

^d Present address: Research Institute for Solid State Physics and Optics, Hungarian Academy of Sciences, POB 49, Budapest H-1525, Hungary

Reprint requests to Dr. U. H.; Fax: +49 381 4986862; E-mail: Hoppe@physik1.uni-rostock.de

Z. Naturforsch. **60a**, 517–526 (2005); received March 22, 2005

X-Ray diffraction, using high-energy photons from a synchrotron, was used to extend the investigation of $(\text{ZnO})_x(\text{P}_2\text{O}_5)_{1-x}$ glasses to samples of ZnO content close to $x = 0.8$ which were obtained by roller-quenching. The isolated PO_4 tetrahedra are surrounded by ZnO_n polyhedra, where Zn–O coordination numbers of ~ 4.5 are determined. The small increase of N_{ZnO} from ~ 4 at metaphosphate composition ($x = 0.5$) to ~ 4.5 is not sufficient to explain the strong increase of the packing density beyond the minimum at $x = 0.5$. The medium-range order was analyzed on the basis of partial $S_{\text{PP}}(Q)$ and $S_{\text{ZnZn}}(Q)$ factors obtained from Reverse Monte Carlo simulations of glasses with $0 \leq x \leq 0.8$. The positions of the first peaks in these factors, the number densities of P and Zn atoms and knowledge of definite P–P and Zn–Zn distances were used to check the applicability of simple models such as the dense packing of uniform P- and Zn-centered spherical environments for glasses with $x = 0.8$ and 0.5 , the packing of corrugated sheets for vitreous P_2O_5 and the packing of phosphate chains for Zn metaphosphate glass.

Key words: X-Ray Diffraction; Glass Structure; Reverse Monte Carlo.

1. Introduction

Special interest in the structure of some binary phosphate glasses originates from early results on the properties of the $(\text{MO})_x(\text{P}_2\text{O}_5)_{1-x}$ series, where glasses with $\text{M} = \text{Be}, \text{Zn}, \text{Mg}$ have been found to show minimum mass densities at metaphosphate composition ($x = 0.5$) [1]. To investigate the structural origin of the density anomalies, several experimental methods were used during the last decades. Numerous investigations were directed to obtain the oxygen coordination numbers of the participating structural groups of either the network forming or the network modifying oxides. Changes of coordination numbers would cause strong packing effects. Most diffraction experiments were made on Zn and Mg metaphosphate glasses. The resulting P–O and Zn–O coordination numbers are four, for example, as reported in [2]. Investigations of anhydrous samples in the ultraphosphate range ($x < 0.5$) became possible with the preparation of the

Zn phosphate glasses in sealed ampoules [3]. In opposite direction, roller quenching techniques allowed the preparation of glassy samples with compositions up to $x \cong 0.8$ [4]. Spectroscopic [3–11] and diffraction [9, 11–14] methods have shown the PO_4 units to be the basic structural groups in the glasses throughout the full range of ZnO content. The units are linked with each other by tetrahedral corners. Changes of numbers of links per PO_4 network unit were investigated by IR and Raman spectroscopy [3, 6, 8] and by ^{31}P magic angle spinning nuclear magnetic resonance (MAS NMR) spectroscopy [4, 9–11]. Double quantum MAS NMR [4] and high performance liquid chromatography [4, 15] were used to extract more details of the links between the PO_4 tetrahedra. However, all these results do not yield any clear explanation for the anomalous behaviour of the mass density mentioned above.

Diffraction was used for determination of the compositional behaviour of the Zn–O coordination num-

bers, N_{ZnO} . Measurements of glasses rich in P_2O_5 content ($x \leq 0.4$) result in N_{ZnO} numbers increasing from four to six with decreasing x [12, 13]. On the other hand, the N_{ZnO} numbers are found not to change for glasses of $0.5 \leq x \leq 0.7$ [11, 14]. The N_{ZnO} are equal to four or little greater than four. The change of N_{ZnO} in the ultraphosphate range explains the decreasing packing densities for glasses with x increasing from ~ 0.33 to ~ 0.5 [12, 16]. This decrease of the packing density corresponds to the plateau of the mass density reported in [1, 3, 8]. On the other hand, the following strong increase of the mass and packing density for $x > 0.5$ [1, 6, 11, 14] is explained with a change of the structural function of the oxygen atoms [12, 16]. The terminal oxygen atoms (O_T) of glasses of $0.33 \leq x \leq 0.5$, i. e. the O atoms not forming P-O-P bridges, are mainly situated in P-O-Zn bridging positions [12, 16]. However, the number of O_T available for coordination of each Zn site decreases with increasing ZnO content. For $x > 0.5$ it decrease to less than four. The Zn^{2+} ions start to share O_T neighbours. This new feature results in increasing numbers of P-Zn distances of ~ 0.32 nm and in new short Zn-Zn distances of ~ 0.33 nm. From these changes an increase of the packing density ensues [17]. The corresponding behaviour was simulated by the Reverse Monte Carlo (RMC) method [17]. Also Molecular Dynamics (MD) work [18] yields the corresponding structural features.

Till now, diffraction was not performed on Zn phosphate glasses with $x > 0.7$, thus, on samples which are only obtained by roller quenching. The present investigation closes this gap. X-Ray diffraction (XRD) experiments performed with high-energy photons from a synchrotron are highly suited for precise determinations of Zn-O coordination numbers [11, 14]. Unfortunately, the available amount of sample material was not sufficient for a parallel neutron diffraction experiment. Thus, only a single set of XRD data is available for the RMC approach which will continue the preceding RMC simulations of the structures of Zn phosphate glasses [17] and of vitreous P_2O_5 [19]. This limitation should not much affect the planned estimations of the change of the spatial distributions of the P and Zn sites with increasing ZnO content. Finally, the medium-range order (MRO) of the RMC model structures of the $(\text{ZnO})_x(\text{P}_2\text{O}_5)_{1-x}$ glasses in a compositional range beginning from the three-dimensional network of vitreous P_2O_5 with three-fold connected PO_4 units ($x = 0$) to a Zn phosphate glass of $x = 0.8$ with merely isolated PO_4 units will be discussed.

2. Experimental

2.1. Sample Preparation

Two samples of $(\text{ZnO})_x(\text{P}_2\text{O}_5)_{1-x}$ glasses with $x = 0.75$ and 0.80 were prepared by roller-quenching. Before quenching the melts were held at 1350 °C in alumina crucibles for 15 min. The number densities of atoms were estimated according to an extrapolation of densities of other samples [11, 14] and to the behaviour of the correlation function, $T(r)$, i. e. the Fourier transform of the scattering data, at small distances which should oscillate around zero (cf. Chapter 3). Number densities of 80 and 82 nm⁻³ revealed to be appropriate for the 75 and 80 mole% samples, respectively.

2.2. X-Ray Diffraction Experiments

The XRD experiments were performed on the BW5 wiggler beamline at the DORIS III synchrotron (Hamburg/Germany), where an energy of incident photons of 122.7 keV ($\lambda = 0.0101$ nm) was used. Powdered material, prepared of the glassy flakes, was loaded into silica capillaries of 2.0 mm diameter, having a wall thickness of 0.01 mm. The detector moves horizontally on a straight line, perpendicularly to the incident beam, scanning the scattering intensity in equidistant steps reaching a maximum scattering angle of 30° . Since the scattering angles and the attenuation of the radiation in the sample material are small, the transmission factors can be assumed to be independent of the angle. Details of such experiments and the corrections are described in [20]. The elastic line and the full Compton profile pass the electronic energy window of the solid-state Ge-detector. Dead-time corrections are made with a parameter τ of 1.08 μs . A fraction of 0.91 of the incident photon beam is polarized horizontally. Corrections are made for background, container scattering, varying sample-detector distance, polarization and absorption. The scattering intensities are normalized to the structure-independent scattering functions, which are calculated by a polynomial approach [21] of tabulated atomic parameters of the elastic scattering factors [22]. Finally, the Compton fractions taken from tabulated data [23] are subtracted and the Faber-Ziman structure factors, $S(Q)$, are calculated [24, 25].

2.3. Reverse Monte Carlo Simulations

The structure of a glass with 80 mole% ZnO is modelled by RMC simulations for comparison with

the RMC structures of Zn phosphate glasses with $x = 0.333, 0.515, 0.640$ and 0.705 [17] and vitreous P_2O_5 [19, 26]. The RMC code used differs from that of McGreevy and Pusztai [27] in handling the coordination constraints. General details are described in [17, 19, 26]. Here the maximum coordination numbers are defined for the P and O sites with $N_{PO} \leq 4$ and $N_{OP} \leq 1$ for a structure with isolated PO_4 units, as it was found for the glass with 80 mole% ZnO (^{31}P MAS NMR [4]). The cubic model box with edge lengths of 2.947 nm contains 2100 atoms, which corresponds to the number density of atoms of 82 nm^{-3} . The total X-ray structure factor of the glass with $x = 0.8$ contains much information about the partial $S_{ij}(Q)$ functions with pairs ij being ZnZn, ZnP, ZnO and PO, but the $S_{PP}(Q)$ and $S_{OO}(Q)$ functions possess only little weight. In order to introduce some information of the $S_{OO}(Q)$ function, the neutron structure factor of the glass with $x = 0.705$ [11] was used. The weight given to the latter structure factor in the RMC runs was distinctly less than that given to the X-ray structure factor. The simulations started with an atomic configuration which was obtained by RMC simulations for the glass with $x = 0.705$ [17]. Appropriate changes were made to the glass composition. Links of PO_4 groups or Zn clusters without PO_4 neighbors were avoided by exchange of P and Zn sites. By this procedure the short Zn-Zn distances are suppressed as much as possible. After several million of accepted moves final models are obtained, where five configurations are accumulated with intervals of hundred thousand accepted moves.

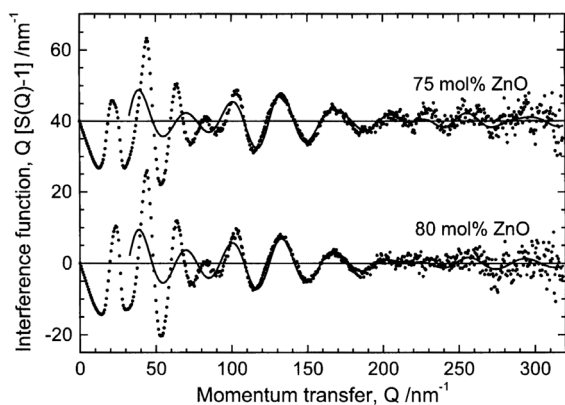


Fig. 1. Interference functions, $Q[S(Q) - 1]$, of the two Zn phosphate glasses studied. The experimental data (dots) are compared with model functions (lines) which are calculated using the parameters resulting from fitting the first-neighbour peaks.

3. Results

3.1. X-Ray Diffraction

The resulting scattering data are plotted in Fig. 1 by means of the weighted interference functions, $Q[S(Q) - 1]$. The experimental data are compared with model functions which are calculated using the parameters of the Gaussian functions obtained by fitting the P-O, Zn-O and O-O first-neighbour peaks (cf. below). Obviously, the scattering information in the high- Q range is merely related with these first-neighbour peaks. Significant oscillations in the experimental data exist up to Q_{\max} of 318 nm^{-1} , though the noise increases drastically for $Q > 250 \text{ nm}^{-1}$. The corresponding correlation functions, $T(r)$, are calculated by Fourier transformations with

$$T(r) = 4\pi r \rho_0 + 2/\pi \int_0^{Q_{\max}} Q \cdot [S(Q) - 1] M(Q) \sin(Qr) dQ, \quad (1)$$

where ρ_0 is the number density of atoms. The Q_{\max} actually used are the upper limits of the $S(Q)$ factors with 318 nm^{-1} , where a damping with a function $M(Q)$ reduces the effects of noise in the high- Q range. The function used is $M(Q) = \sin(\pi Q/Q_{\max})/(\pi Q/Q_{\max})$ [28]. The resulting $T(r)$ functions are shown in the lower part of Figures 2a,b. Other $T(r)$ functions are obtained without damping but using smaller Q_{\max} , 220 and 270 nm^{-1} for the glasses with 75 and 80 mole% ZnO, and are shown in the upper part of the corresponding figures. The use of density values ρ_0 of 80 and 82 nm^{-3} reveals best agreement between the experimental $T(r)$ functions and the model functions in front of the first real distance peak. The parameters of the Gaussian functions approximating the P-O, Zn-O and O-O first-neighbour peaks are obtained by least-squares fitting. P-O and Zn-O peaks are well separated and allow the determination of the coordination numbers free of assumptions. Only the parameters of the small O-O peak, whose distances are due to the edge lengths of the PO_4 tetrahedra, are determined assuming peak position of $\sim 0.252 \text{ nm}$ as obtained for other glasses of this series [11]. The effects of truncation of Fourier transformation at Q_{\max} , (1), and the Q -dependence of the weighting factors are taken into account, as described in [29, 30]. The Marquardt algorithm [31] is applied for the fits where coordination

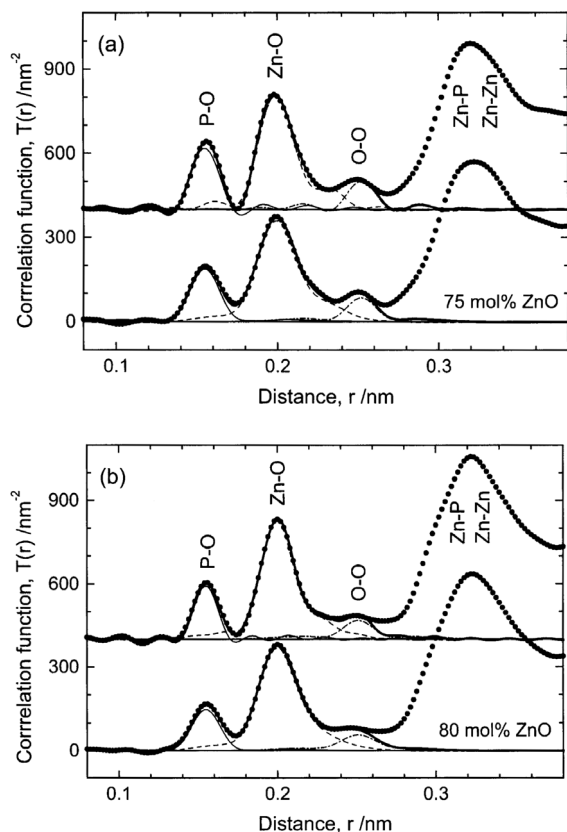


Fig. 2. Correlation functions, $T(r)$, obtained from the data shown in Fig. 1; a) sample with $x = 0.75$; b) sample with $x = 0.80$. Experimental data (dots) are compared with the sum of model peaks (thick solid lines). The different pair distances are given with thin solid lines for P-O, dashed lines for Zn-O and dash-dotted lines for O-O peaks. The model peaks are broadened according to effects of upper limit Q_{\max} , damping $M(Q)$ and Q -dependent weighting factors used in the Fourier transformations, equation (1). The lower functions are obtained with $Q_{\max} = 318 \text{ nm}^{-1}$ and damping according to [28]. The upper functions are obtained with $Q_{\max} = 220$ (a) and 270 nm^{-1} (b) without damping.

numbers, mean distances and full widths at half maximum (fwhm) are the parameters of the model Gaussian functions. At first, the P-O, Zn-O and O-O peaks are tried to fit with single Gaussians. But for taking into account asymmetries of the P-O and Zn-O peaks, the number of Gaussian functions is increased. The distinct Gaussian peaks do not possess much physical meaning. Only the final total coordination numbers and mean distances are relevant. The fits of the $T(r)$ functions are excellent (cf. Figs. 2a,b). The resulting parameters for the two zinc phosphate glasses studied are given in Table 1.

Table 1. Parameters resulting from Gaussian fitting of the P-O, Zn-O and O-O first-neighbor peaks. Distances and full widths at half maximum (fwhm) are given in nm. Parameters marked with asterisks were fixed in the fits.

Sample	Atom pair	Coordination number	Distance	fwhm	Total coordination number	Mean distance
$x = 0.75$	P-O	3.5	0.1545	0.010	4.0 ± 0.1	0.155 ± 0.001
		0.5	0.1585	0.014		
	Zn-O	3.3	0.1975	0.021	4.6 ± 0.3	0.203 ± 0.003
		0.8	0.210	0.020		
		0.5	0.230	0.020		
O-O	3.3	0.252*	0.012	3.3 ± 0.2		
$x = 0.80$	P-O	4.0	0.1548	0.010	4.0 ± 0.1	0.155 ± 0.001
		0.2	0.185	0.015		
	Zn-O	2.8	0.1982	0.018	4.5 ± 0.3	0.203 ± 0.003
		1.0	0.210	0.020		
		0.5	0.225	0.024		
		0.5	0.225*	0.020		
	O-O	3.2	0.251*	0.020	3.2 ± 0.2	

The P-O coordination numbers of both samples studied are four, as expected for PO_4 tetrahedra. This fact confirms that the use of the batch compositions of the melts as the chemical compositions of the glassy samples was justified. The mean lengths of the P-O bonds are $\sim 0.155 \text{ nm}$. The Zn-O coordination numbers are little greater than four with values of 4.6 and 4.5. The contributions to the Zn-O peak at $\sim 0.198 \text{ nm}$ exceeding four are due to a tail which extends up to distances of $\sim 0.24 \text{ nm}$. The coordination numbers belonging to the O-O peak are just greater than three, the value expected for isolated PO_4 units. Each oxygen atom occupying a tetrahedral corner of an isolated PO_4 unit has only three neighbours at distances of $\sim 0.252 \text{ nm}$.

3.2. Reverse Monte Carlo Simulations

Figure 3 shows a comparison of the experimental X-ray structure factors of the series of Zn phosphate glasses and of vitreous P_2O_5 with the corresponding model structure factors obtained by RMC simulations. Agreement of the experimental and model structure factors is a necessary condition of a successful RMC run. Additional constraints, such as minimum separation distances and maximum coordination numbers, are used to create reasonable model structures (cf. Chapter 2.2). The P-O, Zn-O and O-O coordination numbers found in the model configurations of the glass with $x = 0.8$ are 3.7, 4.3 and 3.7, respectively. Obviously, the strong weight of the $S_{\text{ZnO}}(Q)$ function impairs the P atoms to realize the expected N_{PO} numbers of four. This is also due to the missing neutron

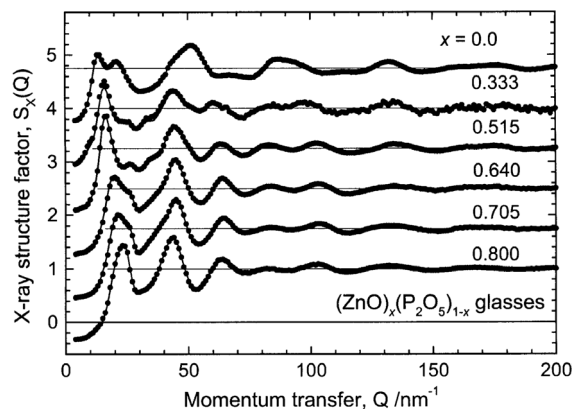


Fig. 3. Comparisons of the experimental X-ray structure factors (dots) with model structure factors (solid lines) calculated from final atomic configurations obtained by RMC simulations. The results shown for vitreous P_2O_5 are taken from [26], results for glasses with $x = 0.333, 0.515, 0.640$ and 0.705 are already shown in [17] and the results for the glass with $x = 0.80$ belong to the present work.

structure factor which would give more weight to the P-O correlations. Fractions of 0.50 and 0.35 of the Zn^{2+} ions occupy positions in ZnO_4 and ZnO_5 polyhedra. The remaining Zn^{2+} are found in less reasonable ZnO_3 groups and in few ZnO_6 groups. The numbers N_{ZnP} , N_{PZn} and N_{ZnZn} of the sample with $x = 0.705$ were extracted with 4.3, 5.1 and 2.6 [17]. Here, for the glass with $x = 0.8$, these numbers are changed to 3.5, 7.0 and 5.4, respectively. Thus, the total numbers of groups adjacent to a given coordination polyhedron increase further to ~ 7 for PO_4 tetrahedra and to ~ 9 for ZnO_n groups. But the increase of the number of neighbouring groups causes only a minor increase of the number density of atoms. The compactation effect is partly compensated by the greater spatial needs of the ZnO_4 tetrahedron in comparison with the needs of a PO_4 tetrahedron.

Since we plan to discuss the behaviour of the spatial distributions of the P and Zn atoms in the full $(ZnO)_x(P_2O_5)_{1-x}$ series of glass structures simulated by the RMC method, it is useful to look at the corresponding scattering intensities. The first diffraction peaks of intensity functions are well suited for estimations of the MRO packing of the P- and Zn-centered oxygen polyhedra. Such estimations are difficult to perform on the basis of only pair distributions. Also it bears some uncertainty to analyse the structure from the positions of the first peaks of the total X-ray scattering intensity. For the glasses under discussion, the $S(Q)$ factors are superpositions of six different partial

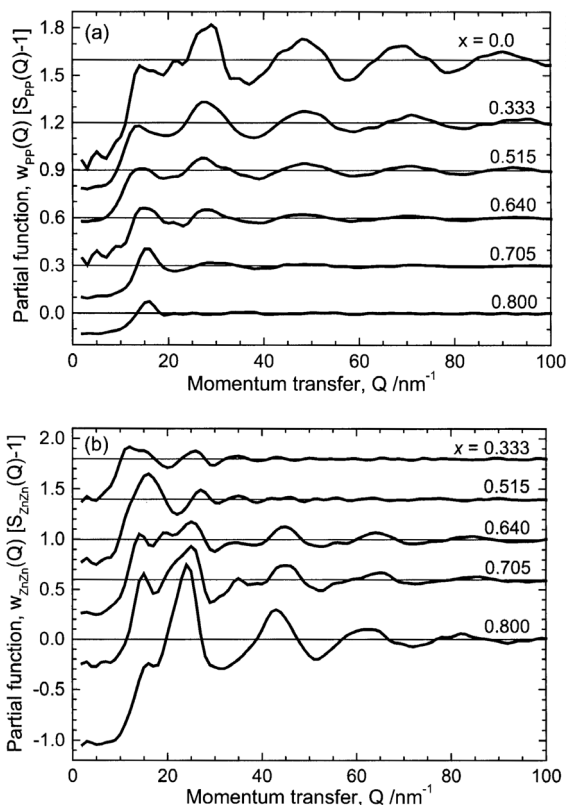


Fig. 4. a) $S_{PP}(Q)$ and b) $S_{ZnZn}(Q)$ structure factors calculated from RMC configurations obtained for vitreous P_2O_5 , i. e. $x = 0.0$ [26], for Zn phosphate glasses with $x = 0.333, 0.515, 0.640, 0.705$ [17], and for a Zn phosphate glass with $x = 0.8$ (this work). The factors are weighted with the corresponding $w_{PP}(Q)$ and $w_{ZnZn}(Q)$ factors; cf. (2) and (3).

contributions with

$$S(Q) = \sum_{ij} w_{ij}(Q) \cdot S_{ij}(Q), \quad (2)$$

where the weighting factors are given by

$$w_{ij}(Q) = (2 - \delta_{ij}) c_i c_j f_i(Q) f_j(Q) / \langle f \rangle^2. \quad (3)$$

c_i is the molar fraction of atomic species i , $f_i(Q)$ is the corresponding scattering amplitude and $\langle f \rangle$ stays for the compositional average of $f_i(Q)$. δ_{ij} is the Kronecker symbol, being unity in case of $i = j$, otherwise it vanishes.

The distributions of the P- and Zn-centered oxygen polyhedra are reflected in the partial $S_{ij}(Q)$ factors with pairs ij being PP or ZnZn. The corresponding functions calculated from the RMC configurations are plotted in Figures 4a,b. The $S_{ij}(Q)$ factors shown are weighted with the corresponding functions $w_{ij}(Q)$.

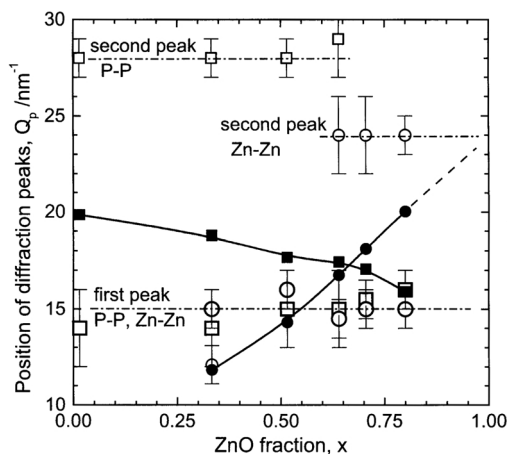


Fig. 5. Positions of the first diffraction peaks of the partial structure factors shown in Figure 4. The peak positions of the $S_{PP}(Q)$ and $S_{ZnZn}(Q)$ factors are indicated with open squares and circles, respectively. Dash-dotted lines indicate their approximate behaviour. The positions of the first diffraction peaks given with solid squares (P) and circles (Zn) are calculated assuming a dense random packing of P- and Zn-centered spherical environments. The peak positions shift continuously due to a continuous change of the number densities of P and Zn atoms.

The $w_{ij}(Q)[S_{ij}(Q) - 1]$ functions shown are the actual contributions to the total X-ray structure factors already presented in Figure 3. The positions of the first diffraction peaks have been determined from the functions shown in Figure 4. The $S_{PP}(Q)$ functions of the samples with $x = 0.705$ and 0.80 show only single first peaks. In case of the other $S_{PP}(Q)$ functions, the height of the second peak exceeds that of the first peak and is no more a simple oscillation following the first peak. Hence, the positions of these second peaks are also relevant. The $S_{ZnZn}(Q)$ function of the sample with $x = 0.5$ shows only a single first peak. In case of the $S_{ZnZn}(Q)$ functions for the glasses of higher ZnO content the second peaks increase. The $S_{ZnZn}(Q)$ function of the sample with $x = 0.333$ shows a new first peak at smaller Q . The positions of the peaks mentioned are given in Figure 5. The peaks do not shift their positions with the changes of the glass composition. But their relative heights change strongly. The peaks disappear completely for a certain change of ZnO content.

4. Discussion

4.1. Short-range Order

The Zn-O coordination numbers corresponding to the peak at ~ 0.195 nm in glasses with $x = 0.5$

were found to be four [2, 11] or little greater than four [14, 32]. The contributions exceeding four are due to distances of ~ 0.22 nm. The results for Zn phosphate glasses with x changing from 0.5 to 0.7 show an increase of the contributions of distances of ~ 0.22 nm with a change of the total N_{ZnO} from 3.9 to 4.3 [11] or from 4.5 to 4.9 [14]. The N_{ZnO} numbers of ~ 4.5 found for the glasses with $x = 0.75$ and 0.8 indicate a further minor increase if these numbers are compared with our earlier results [11]. Also the first prominent Gaussian function used to fit the Zn-O first-neighbour peak shifts to greater distances of ~ 0.198 nm, while this distance is ~ 0.195 nm for glasses with metaphosphate composition [2, 11, 14, 32]. Thus, the small increase of N_{ZnO} is accompanied by an increase of r_{ZnO} . A small additional contribution of shorter distances (0.185 nm), whose origin is not clear, was found in the fit of the $T(r)$ function of the sample with $x = 0.8$ (Table 1). Either these distances, are due to a contamination with crucible material (Al-O distances), or they are due to Zn-O distances of O atoms which are no more members of a PO_4 unit. For glasses with a ZnO content greater than 0.75 such O atoms should exist.

The increase of N_{ZnO} numbers in the range $0.5 \leq x \leq 0.8$ with decreasing number, M_{TO} , of O_T available for coordination of each Zn atom, seems to be an absurd behaviour. Therefore it is remembered that the numbers M_{TO} are comparably great in phosphate glasses [16]. And M_{TO} is exactly four at metaphosphate composition. All O_T are found in P-O-Zn bridging positions if the Zn^{2+} ions form tetrahedra with the four available O_T . The tetrahedral order of the ZnO_4 group is stabilized because the four second atomic neighbours are only PO_4 units. With further decrease of M_{TO} ($M_{TO} = 2/x$) for $x > 0.5$ the Zn atoms start to share some O_T neighbours. The environmental symmetry of the ZnO_4 tetrahedra is destroyed due to new short Zn-Zn separations of lengths similar with those of Zn-P distances. The formation of the ZnO_5 units possessing lower symmetry is getting easier. For part of the Zn sites the ZnO_5 environment is more profitable. The small increase of the Zn-O coordination numbers is not a unique phenomenon. The Ca^{2+} ions forming CaO_6 octahedra are stabilized in a similar way, but for compositions with $x = 0.333$ [12, 16], where M_{TO} is six. With further increase of CaO content an increase of N_{CaO} to seven at metaphosphate composition ensues [12].

In discussions of the distributions of n of the different ZnO_n sites it is not useful to give too much

weight to the results obtained by RMC simulations, though the 50% ZnO_4 and 35% ZnO_5 polyhedra dominating the glass structure for $x = 0.80$ yield a reasonable distribution. The first RMC simulations made for the glasses with $0.5 \leq x \leq 0.7$ ($N_{\text{ZnO}} \approx 4$) [17] resulted in distributions of n with only 50% of the Zn sites having $n = 4$. Subsequently, the RMC runs were repeated where the formation of ZnO_n units with $n > 4$ was handicapped. The fraction of ZnO_4 units increased to 90% of the ZnO_n , which seems to be more reasonable. But the RMC fit of the $S(Q)$ factors was of the same good quality as in the first case. Obviously, the information of the distributions of n is not much constrained in $S(Q)$ data. Note that the RMC configurations give only possible solutions of fitting the $S(Q)$ data. In some details the final configurations might still differ from the real structural behaviour. The RMC method tends to realize little ordered structures in the limits of the constraints if fitting the $S(Q)$ functions. Nevertheless, the next chapter returns to the RMC method again. The spatial orders of the P and Zn sites are discussed.

4.2. Medium-range Order

The P and Zn positions are equivalent to the centers of oxygen polyhedra and, thus, reproduce main information of the MRO. In [17, 33] we used the Bhatia-Thornton formalism [25, 34] to analyse the spatial order of the P and Zn sites. This formalism is well suited for analysing the site distributions irrespective of the P and Zn species and also for the differentiation of random or preferably alternating site occupations (chemical order).

Here, other simple approaches are used: It will be checked if the Q -positions of the first diffraction peaks reproduced by RMC simulations (cf. Fig. 5) agree with those which would follow from some simple approximations of the MRO of glasses. The first model is the dense random packing of P- or Zn-centered spheres. It is assumed that each of the atomic species forms uniform environments whose geometries can be approximated by spheres. Consequently, the characteristic mean P-P or Zn-Zn first-neighbour distances (R_{PP} , R_{ZnZn}) can be calculated from the known number densities of P or Zn atoms. A packing density of $\sim 64\%$, the highest possible for random packing of spheres [35], is assumed. The first diffraction peak of the system is expected at

$$Q_1 \approx 7.7/R_{ii}. \quad (4)$$

The positions Q_1 of first diffraction peaks for the ‘sublattices’ of P or Zn atoms change in opposite direction with increasing x (cf. Fig. 5) because the number density of P atoms decreases while that of Zn atoms increases. A similar model of packing was suggested by Blétry [36]: The same relation between Q_1 and R_{ii} as (4) is valid for an fcc lattice. A minor decrease of 5% for the Q_1 values or increase of R_{ii} values would follow from the higher packing of 74% in the fcc lattice. The behaviour of the MRO of the Zn phosphate glasses does not follow the continuous changes indicated by the model. Only for definite compositions the Q_1 calculated by (4) and the Q_1 simulated by the RMC method are equal. Only these structures will be discussed.

Figure 5 reveals that the first peak of $S_{\text{PP}}(Q)$ for $x \approx 0.8$ and the first peak of $S_{\text{ZnZn}}(Q)$ for $x \approx 0.5$ can be interpreted in the sense of the packing of spheres. The corresponding mean distances R_{PP} and R_{ZnZn} calculated from the number densities of P and Zn atoms are 0.53 and 0.59 nm. The corresponding atomic species form uniform environments for these compositions: In case of $x = 0.8$ all P atoms form isolated PO_4 units [4] surrounded by ZnO_n polyhedra. In case of $x = 0.5$ all Zn atoms form isolated ZnO_4 [17, 33] tetrahedra surrounded by PO_4 tetrahedra. Figure 6 shows the pair distributions $g_{\text{PP}}(r)$ and $g_{\text{ZnZn}}(r)$ obtained by RMC simulations for the glasses with $x = 0.0, 0.515,$ and 0.80 . A first broad peak of P-P distances is found at the expected length (glass with $x = 0.8$). But the calculated R_{ZnZn} is found on the right flank of the peak of Zn-Zn distances ($x = 0.515$). The greater R_{ZnZn} calculated from the density should be due to the lower packing of the Zn environments at metaphosphate composition. The number of first Zn neighbours of the Zn-centered sphere belonging to the Zn-Zn peak ($x = 0.515$) amounts to only ~ 7.5 while the number of first P neighbours of the P-centered sphere ($x = 0.8$) is ~ 11 . It is a property of an ordered (fcc lattice) or disordered packing of spheres, that a considerable change of packing density causes merely minor changes of Q_1 , the position of the first diffraction peak. Thus, estimations of first neighbour distances for a disordered packing starting from the number densities of spheres, not knowing the degree of packing and the dimension of spheres, are not fully conclusive. Earlier [17] we reported calculations of Q_1 by estimation of the dimensions of Zn-centered spheres, using (4), as well. This approach was more successful because reasonable Zn-Zn distances, i.e. the diameters of spheres, were used.

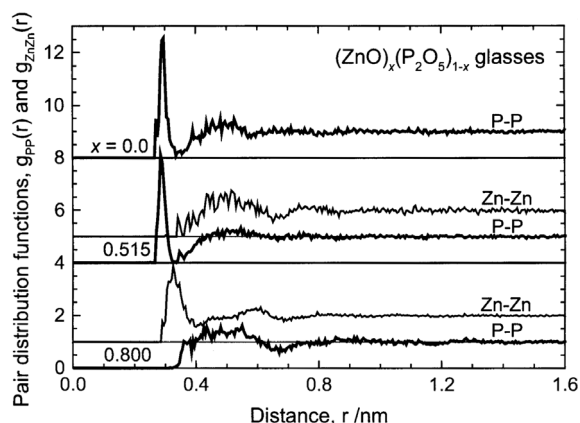


Fig. 6. Pair distribution functions $g_{PP}(r)$ and $g_{ZnZn}(r)$ calculated from RMC configurations for the structure of Zn phosphate glasses with $x = 0.0$ [26], 0.515 [17], and 0.8 (this work).

They were identified in the structures (Fig. 6 [17]). But the packing density of the spheres was not considered.

An extrapolation of Q_1 values in the limit $x \rightarrow 1$ for the $S_{ZnZn}(Q)$ functions is given with the dashed line in Figure 5. It seems that the calculated Q_1 values approach the position of the peak at $\sim 24 \text{ nm}^{-1}$, while the peak at $\sim 15 \text{ nm}^{-1}$ vanishes completely (cf. Fig. 4b). Thus, in the limit of ‘amorphous ZnO’, the packing of ZnO_n units seems to follow the simple model, as well. In opposite direction, for the structure of a glass with $x = 0.333$ (Fig. 5), the calculated Q_1 value approaches the position of a new shoulder found in $S_{ZnZn}(Q)$ (Fig. 4b). We would not interpret this peak in the sense of the simple model of random packing. This shoulder expresses a new Zn-Zn distance typical for ultraphosphate networks [17].

The analysis of total X-ray $S(Q)$ factors shown in Fig. 3 would not allow to extract the specifics of changes of the distributions of the P and Zn sites with increasing ZnO content. But the RMC simulations yield the partial $S_{ij}(Q)$ or $g_{ij}(r)$ functions. These functions reveal the preference for definite P-P and Zn-Zn distances in the MRO throughout the full compositional range of Zn phosphate glasses. The frequencies of these distances change continuously, but not their magnitudes. Thus, the simple models of packing of typical P- or Zn-centered spherical environments are successful only for definite glass compositions.

Two special cases of phosphate structure are considered separately: The structure of vitreous P_2O_5 is formed of three-fold corner-connected PO_4 tetrahedra [19,37]. In earlier interpretations of the peculiar

first diffraction peak of this glass (double peak in the X-ray structure factor) a packing of corrugated sheets was suggested [38]. One of the crystalline modifications consists of corrugated sheets which itself are formed of interconnected six-membered rings of PO_4 tetrahedra [39]. The first peak at $Q_1 \cong 14 \text{ nm}^{-1}$ in the $S_{PP}(Q)$ function (Fig. 4a) is interpreted as the signature of the interlayer spacing D_{sh} with $D_{sh} = 2\pi/Q_1$ where a length of 0.45 nm is calculated. Assuming the sheets to be formed of six-membered rings similar to the crystalline P_2O_5 form III [39], and taking into account the number density of P atoms of the glass (20.63 nm^{-3} [19]), a P-P distance of 0.285 nm is obtained under the assumption of planar layers of interconnected hexagons (honeycomb pattern). On the other hand, a P-P distance of 0.295 nm was extracted by Gaussian fitting of the peak in the correlation function [19]. The difference to 0.285 nm can be explained with the non-planar but wavy character of the real sheets. Thus, the interpretation of the first peak at 14 nm^{-1} in $S_{PP}(Q)$ with an interlayer spacing is justified. Fragments of packed sheets have been found in the RMC configurations of vitreous P_2O_5 [19,26].

Phosphate glasses with metaphosphate composition consist of infinite chains and/or rings of two-fold corner-connected PO_4 tetrahedra [37]. Excluding ring structures and assuming a packing of meandering chains, each chain axis would have six chain neighbours at a mean distance R_{ch} . Since Q_1 is related to the height of an equilateral triangle with the lateral length R_{ch} one obtains $R_{ch} = 4\pi/\sqrt{3}Q_1$. If the first peak at 15 nm^{-1} in $S_{PP}(Q)$ of the Zn metaphosphate glass is interpreted to be caused by a packing of chains, the distance between neighbouring chain axes is obtained as $R_{ch} = 0.48 \text{ nm}$. Now again, using the number density of P atoms in the glass (15.01 nm^{-3} [17]), the mean P-P distance along the chain axes can be calculated. The resulting distance of 0.329 nm is greater than the P-P distance of 0.295 nm found in the RMC configurations [17]. A length smaller than 0.295 nm is expected for meandering chains where P atoms are not arranged in straight lines along the axis. Hence, the large peak at $Q_1 = \sim 15 \text{ nm}^{-1}$ (Fig. 4a) is not caused by the packing of chains. Note that the first peak in $S_{PP}(Q)$ of KPO_3 glass was found at 11 nm^{-1} [33,40], which better matches a model of chain packing. Thus, the phosphate chains of Zn metaphosphate glass do not cause significant interferences due to their packing. Suzuya *et al.* [14] have found a weak shoulder at 10.5 nm^{-1} in the first diffraction peak of the corresponding neutron

structure factor, which could be related with the chain packing. Use of the Bhatia-Thornton formalism [34] has shown that scattering of the P and Zn sites of RMC configurations gives clear indications for a silica-like structure of this glass [17, 33]. The best structural relation of this glass could be made to crystalline β -ZnP₂O₆ [41], whose structure is assumed similar to that of BeP₂O₆ [42]. The PO₄ tetrahedra in these crystals form meandering chains with ZnO₄ tetrahedra connecting four of them with Zn-O-P bridges to form a three-dimensional tetrahedral network similar to a silica polymorph.

5. Conclusions

The diffraction investigations of (ZnO)_x(P₂O₅)_{1-x} glasses are extended to samples with a ZnO content close to $x = 0.8$, which are obtained by roller-quenching. The PO₄ tetrahedra of these glasses are completely surrounded by ZnO_n polyhedra. The Zn-O coordination numbers are found to be ~ 4.5 , which continues the small increase of N_{ZnO} from ~ 4.0 for $x = 0.5$ to ~ 4.3 for $x = 0.7$. This increase of N_{ZnO} is not sufficient to explain the strong increase of the packing density, which rather results from a change of O

atoms in Zn-O-P bridging positions to O atoms shared between several Zn neighbours.

Simple models of the spatial order of the P and Zn sites have been used to analyse the origin of the first diffraction peaks in the $S_{\text{PP}}(Q)$ and $S_{\text{ZnZn}}(Q)$ factors obtained from RMC configurations where the number densities of atoms have been taken into account. The first diffraction peaks do not show a continuous shift, though the atomic density of the glasses changes continuously. The spatial order can be interpreted with a packing of P- or Zn-centered spherical environments only at glass compositions $x \sim 0.8$ for PO₄ tetrahedra surrounded by ZnO_n units, or $x \sim 0.5$ for ZnO₄ tetrahedra surrounded by PO₄ units. In the latter case the packing density is significantly less than the maximum limit of 64%. The first diffraction peak in $S_{\text{PP}}(Q)$ of vitreous P₂O₅ can be interpreted with an interlayer spacing of sheets formed of interconnected six-membered rings of PO₄ units. The corresponding first peak for Zn metaphosphate glass, however, cannot be caused by the packing of the phosphate chains dominating the metaphosphate structures.

Acknowledgements

Great thanks for financial support are expressed to Deutsche Forschungsgemeinschaft (KR 1372/9-1).

- [1] E. Kordes, W. Vogel, and R. Feterowsky, *Z. Elektrochem.* **57**, 282 (1953).
- [2] M. Bionducci, G. Licheri, A. Musinu, G. Navarra, G. Piccaluga, and G. Pinna, *Z. Naturforsch.* **51a**, 1209 (1996).
- [3] A. Barz, K. Meyer, and D. Stachel, *Glastech. Ber.* **68 C1**, 79 (1995).
- [4] B. Tischendorf, J. U. Otaigbe, J. W. Wiench, M. Pruski, and B. C. Sales, *J. Non-Cryst. Solids* **282**, 147 (2001).
- [5] E. C. Onyiriuka, *J. Non-Cryst. Solids* **163**, 268 (1989).
- [6] R. K. Brow, D. R. Tallant, S. T. Myers, and C. C. Phifer, *J. Non-Cryst. Solids* **191**, 45 (1995).
- [7] R. K. Brow, *J. Non-Cryst. Solids* **194**, 267 (1996).
- [8] K. Meyer, *J. Non-Cryst. Solids* **209**, 227 (1997).
- [9] A. Lai, A. Musinu, G. Piccaluga, and S. Puligheddu, *Phys. Chem. Glasses* **38**, 173 (1997).
- [10] J. W. Wiench, M. Pruski, B. Tischendorf, J. U. Otaigbe, and B. C. Sales, *J. Non-Cryst. Solids* **263–264**, 101 (2000).
- [11] G. Walter, U. Hoppe, J. Vogel, G. Carl, and P. Hartmann, *J. Non-Cryst. Solids* **333**, 252 (2004).
- [12] U. Hoppe, G. Walter, R. Kranold, D. Stachel, and A. Barz, *J. Non-Cryst. Solids* **192–193**, 28 (1995).
- [13] U. Hoppe, G. Walter, D. Stachel, A. Barz, and A. C. Hannon, *Z. Naturforsch.* **52a**, 259 (1997).
- [14] K. Suzuya, K. Itoh, A. Kajinami, and C.-K. Loong, *J. Non-Cryst. Solids* **345–346**, 80 (2004).
- [15] B. C. Sales, J. U. Otaigbe, G. H. Bell, L. A. Boatner, and J. O. Ramey, *J. Non-Cryst. Solids* **226**, 287 (1998).
- [16] U. Hoppe, *J. Non-Cryst. Solids* **195**, 138 (1996).
- [17] U. Hoppe, G. Walter, G. Carl, J. Neufeind, and A. C. Hannon, *J. Non-Cryst. Solids* **351**, 1020 (2005).
- [18] B. C. Tischendorf, T. M. Alam, R. T. Cygan, and J. U. Otaigbe, *J. Non-Cryst. Solids* **316**, 261 (2003).
- [19] U. Hoppe, G. Walter, R. Kranold, and D. Stachel, *Z. Naturforsch.* **53a**, 93 (1998).
- [20] H. F. Poulsen, J. Neufeind, H.-B. Neumann, J. R. Schneider, and M. D. Zeidler, *J. Non-Cryst. Solids* **188**, 63 (1995).
- [21] D. Waasmeier and A. Kirfel, *Acta Crystallogr. A* **51**, 416 (1995).
- [22] E. N. Maslen, A. G. Fox, and M. A. O’Kiefe, in: *International Tables for Crystallography, Vol. C* (Ed. A. J. C. Wilson), Kluwer Academic, Dordrecht 1992, p. 476.
- [23] J. H. Hubbell, W. J. Veigle, E. A. Briggs, R. T. Brown, D. T. Cromer, and R. J. Howerton, *J. Phys. Chem. Ref. Data* **4**, 471 (1975).
- [24] T. E. Faber and J. M. Ziman, *Phil. Mag.* **11**, 153 (1965).
- [25] Y. Waseda, in: *The Structure of Non-crystalline Materials*, McGraw-Hill, New York 1980, p. 11–27.

- [26] U. Hoppe, *J. Phys.: Condens. Matter* **12**, 8809 (2000).
- [27] R.L. McGreevy and L. Pusztai, *Molec. Sim.* **1**, 359 (1988).
- [28] E. A. Lorch, *J. Phys. C* **2**, 229 (1969).
- [29] R.L. Mozzi and B.E. Warren, *J. Appl. Crystallogr.* **2**, 164 (1969).
- [30] A. J. Leadbetter and A. C. Wright, *J. Non-Cryst. Solids* **7**, 23 (1972).
- [31] D. Marquardt, *SIAM J. Appl. Math.* **11**, 431 (1963).
- [32] U. Hoppe, R. Kranold, D. Stachel, and J. Neuefeind, *Phosphorus Res. Bull.* **10**, 546 (1999).
- [33] U. Hoppe, G. Walter, R. Kranold, and D. Stachel, *J. Non-Cryst. Solids* **263–264**, 29 (2000).
- [34] A. B. Bhatia and D. E. Thornton, *Phys. Rev. B* **2**, 3004 (1970).
- [35] J. D. Bernal, *Nature* **185**, 68 (1960).
- [36] J. Blétry, *Philos. Mag. B* **62**, 469 (1990).
- [37] J. R. van Wazer, in: *Phosphorus and its Compounds*, Vol. 1, Interscience, New York 1958.
- [38] G. Walter, U. Hoppe, T. Baade, R. Kranold, and D. Stachel, *J. Non-Cryst. Solids* **217**, 299 (1997).
- [39] D. Stachel, I. Svoboda, and H. Fuess, *Acta Crystallogr. C* **51**, 1049 (1995).
- [40] U. Hoppe, G. Walter, D. Stachel, and A. C. Hannon, *Ber. Bunsenges. Phys. Chem.* **100**, 1569 (1996).
- [41] F. L. Katnack and F. A. Hummel, *J. Electrochem. Soc.* **105**, 125 (1958).
- [42] E. Schultz, *Beryllium-Polyphosphate Be(PO₃)₂ III*, Thesis, Christian Albrecht University, Kiel 1974.